

Multipartite quantum resource distillation through local measurement programs

Yan Wang,¹ Shao-Qi Lin,¹ Xi-Nuo Tao,¹ Li-Jiong Shen,¹ Yong-Nan Sun,¹
Ze-Yan Hao,^{2,3,4,*} Kai Sun,^{2,3,4,5} Qi-Ping Su,^{1,†} and Chui-Ping Yang^{1,‡}

¹*School of Physics, Hangzhou Normal University, Hangzhou 310036, China*

²*CAS Key Laboratory of Quantum Information, University of Science and Technology of China, Hefei 230026, China*

³*Anhui Province Key Laboratory of Quantum Network,*

University of Science and Technology of China, Hefei 230026, China

⁴*CAS Center for Excellence in Quantum Information and Quantum Physics,*

University of Science and Technology of China, Hefei 230026, China

⁵*Hefei National Laboratory, University of Science and Technology of China, Hefei 230088, China*

Distributed quantum resources in practical multi-user quantum networks are inevitably degraded by environmental noise, channel loss, and device-induced imperfections. To address these issues, quantum resource distillation offers a fundamental approach to recovering stronger resources from imperfect states. However, conventional implementations often require additional copies, dedicated physical filtering elements, or restrict to bipartite systems, posing challenges for scalable multipartite networks. Here, we introduce the method of quantum resource distillation based on the local measurement program (LMP), which transfers completely positive maps into programmable measurement processes. We experimentally demonstrate the performance of resource distillation through LMP in both bipartite and tripartite photonic systems, including the activation and enhancement of multipartite steering configurations. To demonstrate the flexibility and extensibility of the LMP framework, we also show that virtual resource distillation can be naturally reformulated within it. Our results establish a programmable and experimentally economical approach for distilling quantum resources in multipartite and higher-dimensional systems, thereby providing a practical route toward scalable quantum networks.

I. INTRODUCTION.

Quantum resources shared across distant nodes are essential for quantum information science [1] and drive genuine advantages in quantum information processing, e.g., quantum teleportation [2, 3], quantum-enhanced sensing [4], long-distance and secure communication [5], and scalable quantum computing [6]. In realistic scenarios, quantum resources are inevitably exposed to environmental disturbances that induce decoherence [5, 7]. Beyond merely degrading entanglement [8], such noise can also alter directional quantum correlations like quantum steering [9], thereby reshaping which parties still share usable quantum resources. This motivates experimentally feasible methods capable of recovering and purifying useful quantum correlations [10–15], paving the way for more reliable quantum technologies [16–22].

Quantum resource distillation provides a route to recovering stronger nonclassical correlations from imperfect resources [23]. The standard multi-copy protocols rely on additional noisy pairs and use entangling operations to postselect fewer outputs with enhanced entanglement [24, 25], but these requirements become increasingly demanding when scaling to multipartite or high-dimensional systems [26]. More broadly, the distillation protocol can also be formulated as a probabilistic state transformation that enhances the operationally useful correlations of an imperfect resource [27]. Within this perspective, local filtering implements a trace-nonincreasing and completely positive (CP) map on the target state and retains only successful events [28–33].

Such filtering transformations can reveal hidden nonclassical correlations and have been extended from entanglement to steering distillation [34–37]. However, physical local filters are usually implemented by inserted, often fixed, optical elements or specific operations, so each target CP map requires a corresponding hardware configuration and introduces additional loss, alignment sensitivity, and calibration overhead [29–31].

In parallel, virtual resource distillation has been proposed and experimentally demonstrated to reproduce the statistics of target resource transformations without physically preparing the distilled state [38–40]. It offers a different route, yet the existing demonstrations remain formulated as specific statistical reconstructions rather than as a general programmable measurement implementation of local CP maps [40]. Moreover, recent work on temporal asymmetry in entanglement distillation [26] has shown that the choice and ordering of local operations can fundamentally determine whether distilled resources surpass classical thresholds in downstream protocols such as quantum teleportation, underscoring the need for versatile control over the choice and ordering of local operations. Therefore, a unified and programmable framework is still lacking for transferring local CP maps to local measurement procedures, so as to reproduce the same postselected distillation statistics without physically inserting the corresponding state transformation modules.

Here we develop the local measurement program (LMP) for quantum resource distillation, which implements the effect of local CP maps through programmable measurements rather than dedicated entangling gates or

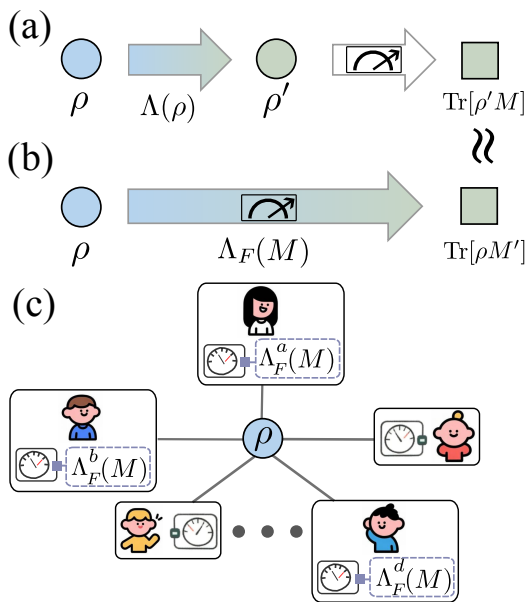


Fig. 1. **Schematic illustration.** (a) The local filtering distillation is constructed through performing local operations $\Lambda(\rho)$ on the initial state ρ . (b) Local measurement program (LMP) distillation implements the filtering map on the measurement basis in $\Lambda_F(M)$. (c) LMP distillation in multipartite systems with local operations selectively performing on i -th partite $\Lambda_F^i(M)$ ($i \in \{a, b, d\}$).

physical local filters. We experimentally demonstrate the LMP framework in both bipartite and tripartite photonic systems under asymmetric noise, achieving distillation of both entanglement and steering, and revealing the hierarchical and directional transformation of tripartite steering correlations. We also show that recently proposed virtual resource distillation can be reformulated within the same LMP picture, establishing a flexible route to resource distillation in multipartite and high-dimensional quantum systems. Our method reduces experimental complexity and system errors, making resource distillation naturally compatible with scalable, multi-user quantum network architectures.

II. THEORETICAL FRAMEWORK.

As for the local filtering distillation in Fig. 1(a), the transformation is typically represented by a CP, trace-nonincreasing map Λ that acts on the input state ρ , with the postselected output state given by

$$\rho' = \Lambda(\rho) = \frac{F\rho F^\dagger}{\text{Tr}[F\rho F^\dagger]}, \quad (1)$$

where $F = \bigotimes_{j \in \mathcal{S}} F_j$ with F_j acting on the j th local subsystem, and the resulting state ρ' exhibits enhanced quantum resources (e.g., entanglement and steerability)

[28–31]. Such a map realizes quantum resource distillation by filtering out unwanted components locally, with a success probability given by $\text{Tr}(F\rho F^\dagger)$. The corresponding measurement probability is

$$\text{Tr}[M_k \rho_F] = \frac{\text{Tr}[M_k F \rho F^\dagger]}{\text{Tr}[F \rho F^\dagger]}. \quad (2)$$

However, physically implementing local filters in Eq. (1) requires fixed optical elements that must be fabricated and aligned with high precision, making the protocol inflexible and increasingly demanding in multipartite or high-dimensional systems.

Motivated by these constraints, we construct the local measurement program (LMP) to distill quantum resources by equivalently transferring the action of the filtering map from the quantum state to the measurement operators, as illustrated in Fig. 1(b). Instead of physically applying F to the quantum state, one can equivalently transform the measurement effects via the Heisenberg-picture dual map [41]

$$\tilde{M}_k \Rightarrow \Lambda_F^\dagger(M_k) = F^\dagger M_k F, \quad (3)$$

with the normalized probability $p(k|\rho_F) = \frac{\text{Tr}(\rho \tilde{M}_k)}{\sum_j \text{Tr}(\rho M_j)} = \frac{\text{Tr}(\rho F^\dagger M_k F)}{\text{Tr}(\rho F^\dagger F)}$. This establishes the central principle of the LMP: embedding the filter operation into the measurement procedure. More details of the LMP operation are provided in Sec. S1 of the Supplementary Material (SM) [42].

More generally, for multipartite or higher-dimensional systems, the LMP protocol can be applied locally to each subsystem by transferring the corresponding local filtering operation to the measurement stage. When the local filter is selectively applied to the i th subsystem, as illustrated in Fig. 1(c), its effect is absorbed into the corresponding local measurement via Eq. (3), while the measurement operators on all other subsystems remain unchanged. Compared with approaches acting directly on quantum states, the LMP avoids physically inserting and aligning multiple filtering elements across different subsystems, substantially simplifying the experimental apparatus. This programmable flexibility becomes essential when the ordering and selection of local operations fundamentally determine whether distilled resources can surpass classical thresholds in quantum information tasks [26], highlighting a key scalability and feasible advantage of the LMP for complex quantum systems.

III. EXPERIMENTAL SETUP.

The illustration of our experimental setup is depicted in Fig. 2(a). The bipartite state is generated by a biphoton entanglement source in the form of $|\Phi(\theta)_b\rangle = \cos\theta |H_s H_i\rangle + \sin\theta |V_s V_i\rangle$ [43, 44], where the subscript

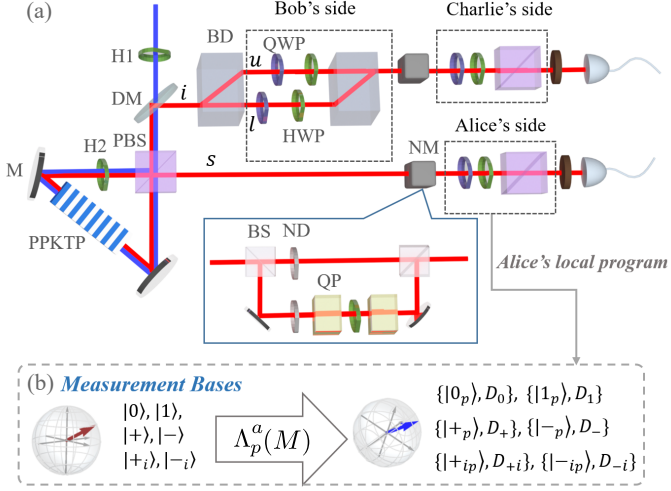


Fig. 2. **Illustration of experiment.** (a) Pairs of entangled photons ($|\Phi(\theta)_b\rangle$) are generated via parametric down-conversion in a periodically poled potassium titanyl phosphate (PPKTP) crystal, with one output sent to beam displacer (BD) to further prepare tripartite states ($|\Phi(\theta)_t\rangle$). The noise module (NM) placed on Alice and Charlie's sides are detailed in the blue box. Three dotted boxes are the measurement apparatus including quarter-wave plate (QWP), half-wave plates (HWP), a BD or a polarized beam splitter (PBS). DM: dichroic mirror, ND: neutral density filter, M: mirror, BS: beam displacer, QP: quartz plate, IF: interference filters. (b) The concept of Alice's local program is to rotate the measurement bases from $\{|0\rangle, |1\rangle, |+\rangle, |-\rangle, |+i\rangle, |-i\rangle\}$ to $\{|0_p\rangle, |1_p\rangle, |+_p\rangle, |-_p\rangle, |+_{ip}\rangle, |-_{ip}\rangle\}$ along with the normalized coefficients $D_0, D_1, D_+, D_-, D_{+i}$ and D_{-i} , according to the operator F_a in (6).

s (i) represents the signal (idler) photon, and H (V) is the horizontal (vertical) polarization. The parameter θ can be tuned by the half-wave plate (HWP) H1 in Fig. 2(a). For the tripartite case, the computational bases are encoded in photons' polarization and path degrees of freedom as the form: $|\Phi(\theta)_t\rangle = \cos\theta |H_s H_i u\rangle + \sin\theta |V_s V_i l\rangle = \cos\theta |000\rangle + \sin\theta |111\rangle$, where polarization information H (V) and path modes u (l) are encoded 0 (1) [45]. The local noise module (NM) with tunable strength is further inserted via the unbalanced interferometer, resulting in the bipartite and tripartite states as

$$\rho_b = \eta |\Phi(\theta)_b\rangle \langle \Phi(\theta)_b| + \frac{(1-\eta)}{2} \mathbb{1}_A \otimes \rho_C^\theta, \quad (4)$$

and

$$\rho_t = \eta |\Phi(\theta)_t\rangle \langle \Phi(\theta)_t| + \frac{(1-\eta)}{2} \mathbb{1}_A \otimes \rho_{BC}^\theta, \quad (5)$$

with the ratio (η) controlled by the neutral density filters (NDs), $\rho_C^\theta = \text{Tr}_A[|\Phi(\theta)_b\rangle \langle \Phi(\theta)_b|]$ and $\rho_{BC}^\theta = \text{Tr}_A[|\Phi(\theta)_t\rangle \langle \Phi(\theta)_t|]$. The measurement process consists of two polarization analyzers (on Alice and Charlie's sides) in the bipartite case, while an additional path analyzer (on Bob's side) is introduced in the tripartite case.

Photons are collected by the single-photon detector after an interference filter with a 3-nm bandwidth and sent the output signal to a further coincidence device. We then perform the standard quantum state tomography for each experimentally prepared state [46], with the average fidelity for all bipartite and tripartite states 0.972(4) and 0.963(6). More experimental details are in S2 of the SM [42].

The distillation process via LMP then works on the measurement device with the schematic principle shown in the dashed box of Fig. 2(b). Here, we illustrate the LMP through an effective local filtering operation on Alice's side as

$$F_a = \begin{pmatrix} \sin\theta & 0 \\ 0 & \cos\theta \end{pmatrix}, \quad (6)$$

which is equivalent, up to an irrelevant overall normalization factor, to the inverse Schmidt-coefficient filter and satisfies $F_a^\dagger F_a \leq \mathbb{I}$. Moreover, the form of F_a is explicitly determined by the state parameter θ , while independent of η . The initial measurement bases (before applying LMP) are the eigenstates of three Pauli matrices, respectively represented in the basis as $|0(1)\rangle = |H(V)\rangle$, $|+(-)\rangle = |H\rangle \pm |V\rangle$ and $|+i(-i)\rangle = |H\rangle \pm i|V\rangle$. Alice's LMP will update the measurement bases according to Eq. (3), resulting the new measurement bases (after applying LMP) as $|0_p(1_p)\rangle = |H(V)\rangle$, $|+_p(-_p)\rangle = \sin\theta |H\rangle \pm \cos\theta |V\rangle$ and $|+_{ip}(-_{ip})\rangle = \sin\theta |H\rangle \pm i\cos\theta |V\rangle$ along with the normalized coefficients D_k ($k \in \{0, 1, +, -, +i, -i\}$). We then utilize the local program on Alice's side, which can replace the physically optical components required from local operations by employing the basis rotation and subsequent data processing. The local program is also feasible and extendable to other parties, i.e., Bob or Charlie's sides.

IV. EXPERIMENTAL RESULTS.

We first prepare series of bipartite states through subjecting to fixed asymmetric noise $\eta_b = 40\%$ with varying $\theta_b \in (0, \pi/2)$, and fixed $\theta_b = \pi/8$ with varying asymmetric noise $\eta_b \in (0, 1)$. The LMP is further applied to realize the distillation process with the experimental results denoted as solid and hollow markers representing the degree of entanglement (C) and steerability (S), which is demonstrated by $C > 0$ [47] and $S > 0$ [48]. Here, the steering parameter S is quantified from two directions, where S_{ab} denotes steerability from Alice to Bob and S_{ba} means Bob to Alice. The detailed calculations of the entanglement and steering criteria are in the S3 of SM [42]. The distillation performance of LMP in bipartite system is shown in Fig. 3.

To obtain updated measurement bases and their normalization factors, the LMP adapts to different values

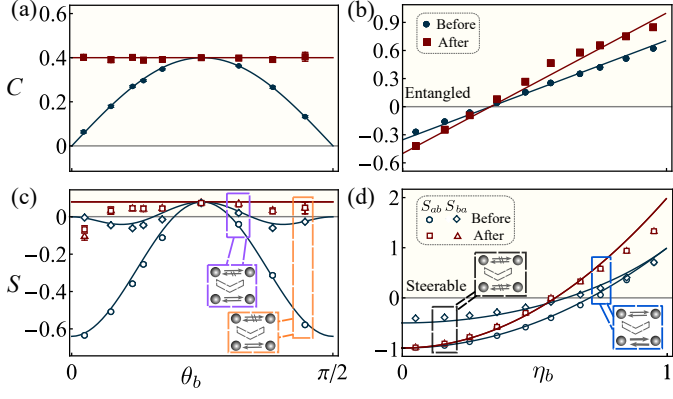


Fig. 3. **Experimental results in the bipartite case.** The blue circles and rhombuses (red squares and triangles) represent before (after) distillation process. The solid and hollow markers respectively represent the concurrence (C) and steerability (S) of the bipartite states, where S_{ab} (S_{ba}) are the steerability from Alice to Bob (Bob to Alice). The solid lines are the corresponding theoretical analysis. The yellow regions are denoted the entangled regions in (a) and (b), and the steerable regions in (c) and (d). The dashed boxes described the steering transformations. All errors are calculated assuming Poissonian statistics.

of the parameter θ under a fixed noise module by updating the corresponding measurement bases and normalization factors. For states with fixed θ , the same measurement bases and normalization are used for different noise ratios. Owing to the hierarchical structures of quantum steering, we observe three distinct distillation scenarios, highlighted by the dashed boxes in Fig. 3, i.e., the enhancement of initially two-way steerable states (the blue box), the conversion of one-way to two-way steerable states (the purple box), and the activation of previously unsteerable to two-way steerable states (the orange box). Moreover, the distillation effect of LMP would become ineffective (in black box) when varying parameter η in (b) and (d), primarily because the mathematical form of the local filter employed in Eq. (6) fails to purify the system state unless the parameter η exceeds a critical threshold. In this situation, only the initial states containing entanglement and steerability can be successfully distilled. Meanwhile, the observation that quantum steering requires higher threshold compared with that of entanglement reveals the hierarchical relationship between these quantum resources.

We then characterize the distillation effect of LMP in the tripartite system in Fig. 4, including fixed asymmetric noise $\eta_t = 10\%$ with varying $\theta_t \in (0, \pi/2)$ and fixed $\theta_t = \pi/9$ with varying asymmetric noise $\eta_t \in (0, 1)$. In the tripartite case, the entanglement (steering) is verified with $W(S) < 0$ [45, 49]. Here, the tripartite quantum steering S is calculated in both one-sided ($S_{a|bc}$) and two-sided ($S_{ab|c}$) device independent scenarios. The detailed

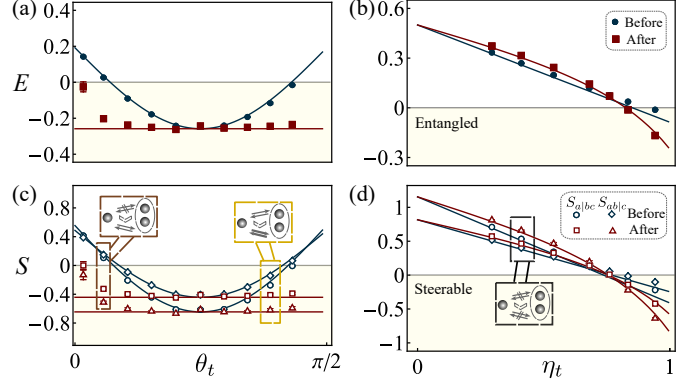


Fig. 4. **Experimental results in the tripartite case.** The blue circles and rhombuses (red squares and triangles) represent experimental results before (after) distillation, and the solid and hollow markers respectively represent the entanglement (E) and steering witness (S), along with the theoretical analysis in solid lines. The parameters $S_{a|bc}$ ($S_{ab|c}$) in (c) and (d) denote the steering witness from Alice to Bob and Charlie (Alice and Bob to Charlie), where the steerability transformations are denoted in the dashed boxes. The yellow background is corresponding to entangled regions in (a) and (b), and steerable regions in (c) and (d). All errors are calculated under Poissonian statistics.

calculations of the entanglement and steering criteria are in S4 of the SM [42]. Similarly, the distillation protocol works across different values of θ_t , while for fixed θ_t and varying η_t , successful distillation is observed only when the noise ratio remains below a threshold. In particular, we observe different configurations of multipartite steering distillation, including the enhancement and activation of steerability in the yellow and brown boxes from both one-sided and two-sided device independent scenarios. The black box, by contrast, denotes the persistence of unsteerable states after the LMP processing. These observations demonstrate that the LMP can flexibly manipulate multipartite steering configurations and be generalized to multipartite systems.

Our experimental results in both bipartite and tripartite systems show agreement with the theoretical predictions, confirming the effectiveness of the LMP in purifying quantum resources and providing a feasible approach for distilling genuine multipartite entanglement and quantum steering. The deviations between experimental results and the theoretical analysis primarily stems from fluctuations of the entangled source, small calibration errors in the wave plates and the imperfections of our measurement apparatus. Notably, as the initial quantum resource decreases, i.e., the parameter θ approaches 0 or $\pi/2$, the beforementioned experimental errors are amplified, making the distillation process more sensitive to such experimental errors and thereby degrading the distillation performance.

Moreover, we reformulate the recently proposed virtual

resource distillation [39, 40] in terms of the LMP framework, where a noisy Werner state is virtually distilled through a linear combination of measurement statistics. The desired virtual transformation can be decomposed into CP branches, $\sum_i \Lambda_i(\Psi^-) = \rho_\eta = (\mathbb{I}_4 - |\Psi^-\rangle\langle\Psi^-|)/3$, where $\Lambda_1(\Psi^-) = \Psi^+/3$, $\Lambda_2(\Psi^-) = \rho_{00}/3$, and $\Lambda_3(\Psi^-) = \rho_{11}/3$ [40]. Instead of physically implementing these branches to the quantum state, LMP applies their dual action to the measurement operators, and the local state $|\phi_\mu\rangle$ after applying local operator $F_{i,\mu}$ is programmed as $F_{i,\mu}^\dagger |\phi_\mu\rangle$ after normalization, with the resulting programmed bases and coefficients for all three branches are summarized in Table I. For example, in the Λ_3 branch, the local operator on Bob's side is $F_{3,B} = |1\rangle\langle 1|$, so an original measurement state such as $|R\rangle$ is programmed as $F_{3,B}^\dagger |R\rangle \propto |1\rangle$ after normalization, with the corresponding LMP coefficient $D_R = 1/\sqrt{2}$ compensating the branch success probability. Therefore, the measurement statistics with the LMP program gives the identical output as first applying the corresponding map and then performing the original measurements [40]. In this sense, the above transformation is absorbed into the measurement process, and the same statistics can be obtained through programmed local measurement bases and classical normalization, without implementing additional state-transformation modules as in Ref. [40] and providing a more economical and experimentally accessible way to reproduce the desired virtual distillation effect.

More generally, the LMP shows that the desired distillation effect can be realized by selecting the proper local program. By changing the programming measurement bases and normalization coefficients, different effective local CP maps and channels can be implemented. This programmability allows the same framework to emulate local filtering operations, replacement channels, and other branch-wise CP transformations, indicating its flexibility for multipartite and higher-dimensional quantum systems.

Alice							Bob					
$ 0\rangle$	$ 1\rangle$	$ +\rangle$	$ -\rangle$	$ R\rangle$	$ L\rangle$		$ 0\rangle$	$ 1\rangle$	$ +\rangle$	$ -\rangle$	$ R\rangle$	$ L\rangle$
Λ_1	$ 0\rangle$	$ 1\rangle$	$ +\rangle$	$ -\rangle$	$ R\rangle$	$ L\rangle$	$ 0\rangle$	$ 1\rangle$	$ -\rangle$	$ +\rangle$	$ L\rangle$	$ R\rangle$
Λ_2	$ 1\rangle$	$ 0\rangle$	$ +\rangle$	$ -\rangle$	$ L\rangle$	$ R\rangle$	$ 0\rangle$	$ 0\rangle$	$ 0\rangle$	$ 0\rangle$	$ 0\rangle$	$ 0\rangle$
Λ_3	$ 1\rangle$	$ 0\rangle$	$ +\rangle$	$ -\rangle$	$ L\rangle$	$ R\rangle$	$ 1\rangle$	$ 1\rangle$	$ 1\rangle$	$ 1\rangle$	$ 1\rangle$	$ 1\rangle$
	D_0	D_1	D_+	D_-	D_R	D_L	D_0	D_1	D_+	D_-	D_R	D_L
Λ_1	1	1	1	1	1	1	1	1	1	1	1	1
Λ_2	1	1	1	1	1	1	$\sqrt{2}$	0	$1/\sqrt{2}$	$1/\sqrt{2}$	$1/\sqrt{2}$	$1/\sqrt{2}$
Λ_3	1	1	1	1	1	1	0	$\sqrt{2}$	$1/\sqrt{2}$	$1/\sqrt{2}$	$1/\sqrt{2}$	$1/\sqrt{2}$

TABLE I. Decomposition of the map $\sum_i \Lambda_i(\Psi^-) = \rho_\eta = (\mathbb{I}_4 - |\Psi^-\rangle\langle\Psi^-|)/3$, the corresponding operators and parameters.

V. CONCLUSIONS.

In this work, we propose and demonstrate the resource distillation through LMP protocols in both bipartite and tripartite cases. We observe the effect of purification through entanglement and diverse transformations of steering configurations enabled by the directional structures of quantum steering. Our results indicate that the LMP framework exhibits good adaptability across different quantum systems, while preserving scalability independent of the system size. This would pave the way for resource distillation in more robust and large-scale multipartite quantum networks [50–52].

Using the method outlined in Eq. (3), we further reformulate the virtual resource distillation as a local measurement program, enabling the required experimental apparatus to be replaced by a program applicable solely at the measurement process. This approach demonstrates the flexibility of our local measurement program, which can implement the desired quantum operation by appropriately redefining the measurement basis according to the structure of the corresponding completely positive map. Moreover, by effectively transferring the action of local CP maps onto the measurement settings, the LMP framework can be extended to other classes of local operations and more general CP maps like noise channels and POVM map[53–55]. The LMP implementation provides a broadly applicable route for quantum resource manipulation [56–58].

VI. ACKNOWLEDGMENTS

This work was supported by the National Natural Science Foundation of China Grants No. 12404403 and 123B2067, Zhejiang Provincial Natural Science Foundation of China Grant No.LQN25A040018, National Key Research and Development Program of China (Grant No. 2024YFA1408900), Hangzhou Leading Youth Innovation and Entrepreneurship Team project Grant No. TD2024005.

VII. DETAILS OF LOCAL PROGRAM OPERATION

For a local projective measurement $M_\phi = |\phi\rangle\langle\phi|$ and a CP operation \mathcal{F} , the transformed measurement effect can be written as

$$\mathcal{F}^\dagger M_\phi \mathcal{F} = r_\phi |\phi_{\mathcal{F}}\rangle\langle\phi_{\mathcal{F}}|, \quad (7)$$

where

$$|\phi_{\mathcal{F}}\rangle = \frac{\mathcal{F}^\dagger |\phi\rangle}{\sqrt{\langle\phi|\mathcal{F}\mathcal{F}^\dagger|\phi\rangle}}, \quad r_\phi = \langle\phi|\mathcal{F}\mathcal{F}^\dagger|\phi\rangle. \quad (8)$$

Accordingly, the filtered measurement probability can be obtained from the original local state ρ_L as

$$\text{Tr}[M_\phi \rho_{\mathcal{F}}] = D_{\mathcal{F}} \text{Tr}[\langle \phi_{\mathcal{F}} | \rho_L | \phi_{\mathcal{F}} \rangle], \quad (9)$$

where $\rho_{\mathcal{F}} = \mathcal{F} \rho_L \mathcal{F}^\dagger / \text{Tr}[\mathcal{F} \rho_L \mathcal{F}^\dagger]$ is the locally filtered state of the subsystem on which the local filter operation acts. In practice, this means that the original measurement basis $|\phi\rangle$ is replaced by the updated basis $|\phi_{\mathcal{F}}\rangle$, while the corresponding outcome is renormalized by the normalization factor

$$D_{\mathcal{F}} = \frac{r_\phi}{\text{Tr}[\mathcal{F} \rho_L \mathcal{F}^\dagger]}. \quad (10)$$

In a practical experimental realization, taking the projective measurement as an illustrative example, the procedure can be implemented as follows: (i) The user first characterizes the local reduced state ρ_L of the subsystem, for example through local quantum state tomography. The local operation \mathcal{F} , which is chosen to enhance the desired resource correlations with other parties, can then be determined and further optimized through a feedback mechanism established from the measurement outcomes. (ii) The user inputs \mathcal{F} together with the original projective measurement basis $|\phi\rangle$ and the characterized local state ρ_L into a programmable module. The module incorporates the completely positive transformation into the measurement process and generates the updated measurement basis $|\phi_{\mathcal{F}}\rangle$ together with the normalization factor $D_{\mathcal{F}}$. (iii) The user then performs the measurement using the newly constructed basis $|\phi_{\mathcal{F}}\rangle$ and obtains the corresponding outcomes. These outcomes are multiplied by the normalization factor $D_{\mathcal{F}}$, yielding the final measurement results, which reproduce the effect of the completely positive map at the measurement level.

As a result, the LMP substantially reduces the need for additional physical filtering elements and provides a flexible route for implementing resource distillation in multipartite and higher-dimensional quantum systems.

VIII. CRITERION OF QUANTUM ENTANGLEMENT AND STEERING IN BIPARTITE SYSTEMS

In bipartite case, the degree of entanglement is quantified through concurrence $C = \max\{0, \Lambda = \lambda_1 - \lambda_2 - \lambda_3 - \lambda_4\}$ with λ_i corresponding to the decreasing eigenvalues of Hermitian matrix $\rho(\sigma_y \otimes \sigma_y) \rho^*(\sigma_y \otimes \sigma_y)$ [47]. EPR steering criteria is based on local uncertainty relations in three-measurement settings $\{\vec{x}, \vec{y}, \vec{z}\}$, where Alice is able to steer Bob if the inequality

$$\sum_i \delta^2(\alpha_i A_i + B_i) \geq \min_{\rho_B} \sum_i \delta^2(B_i) \quad (11)$$

is violated, with the variance of measurement outcomes δ and $\alpha_i = -(\langle A_i B_i \rangle - \langle A_i \rangle \langle B_i \rangle) / \delta^2(A_i)$ [48]. Here, we use

the steering parameter $S_{ab} = 2 - \sum_i \delta^2(\alpha_i A_i + B_i) > 0$ demonstrates Alice could steer Bob, and $S_{ab} \leq 0$ means Alice can't steer Bob under three-setting measurements.

IX. CRITERION OF QUANTUM ENTANGLEMENT AND STEERING IN TRIPARTITE SYSTEMS

As for the tripartite case, the entanglement witness $W = \frac{3}{4} \mathbb{1} - P_{GHZ}$ is utilized with the projector $P_{GHZ} = |GHZ\rangle \langle GHZ|$, $|GHZ\rangle = (|000\rangle + |111\rangle) / \sqrt{2}$ and the identity matrix $\mathbb{1}$ [49]. The entanglement witness $W < 0$ indicates the presence of entanglement.

The tripartite EPR steering is calculated in two different scenarios, i.e., the one-sided device-independent (1SDI) and two-sided device-independent (2SDI) cases [45]. In 1SDI scenario, only Alice's measurement device is untrusted while Bob and Charlie are trusted, where the steerability from Alice to Bob and Charlie is denoted as $\mathcal{S}_{a|bc} = 1 + 0.1547 \langle Z_B Z_C \rangle - (\langle A_2 Z_B \rangle + \langle A_2 Z_C \rangle + \langle A_0 X_B X_C \rangle - \langle A_0 Y_B Y_C \rangle - \langle A_1 X_B Y_C \rangle - \langle A_1 Y_B X_C \rangle) / 3$. The steering parameter $\mathcal{S}_{a|bc} > 0$ indicates that Alice can steer the joint state of Bob and Charlie. In 2SDI scenario, Alice and Bob's measurement device are untrusted meanwhile Charlie are trusted, $\mathcal{S}_{ab|c} = 1 - 0.1831 (\langle A_2 B_2 \rangle + \langle A_2 Z \rangle + \langle B_2 Z \rangle) + 0.2582 (-\langle A_0 B_0 X \rangle + \langle A_0 B_1 Y \rangle + \langle A_1 B_0 Y \rangle + \langle A_1 B_1 X \rangle)$. The steering parameter $\mathcal{S}_{ab \rightarrow c} > 0$ indicates that Alice and Bob can jointly steer Charlie's state.

* hzy0526@mail.ustc.edu.cn

† sqp@hznu.edu.cn

‡ yangcp@hznu.edu.cn

- [1] Otfried Gühne, Erkki Haapasalo, Tristan Kraft, Juha-Pekka Pellonpää, and Roope Uola, Colloquium: Incompatible measurements in quantum information science, *Rev. Mod. Phys.* **95**, 011003 (2023).
- [2] Charles H. Bennett, Gilles Brassard, Claude Crépeau, Richard Jozsa, Asher Peres, and William K. Wootters, Teleporting an unknown quantum state via dual classical and einstein-podolsky-rosen channels, *Phys. Rev. Lett.* **70**, 1895–1899 (1993).
- [3] Xiao-Min Hu, Yu Guo, Bi-Heng Liu, Chuan-Feng Li, and Guang-Can Guo, Progress in quantum teleportation, *Nat. Rev. Phys.* **5**, 339–353 (2023).
- [4] C. L. Degen, F. Reinhard, and P. Cappellaro, Quantum sensing, *Rev. Mod. Phys.* **89**, 035002 (2017).
- [5] Koji Azuma, Sophia E. Economou, David Elkouss, Paul Hilaire, Liang Jiang, Hoi-Kwong Lo, and Ilan Tzitrin, Quantum repeaters: From quantum networks to the quantum internet, *Rev. Mod. Phys.* **95**, 045006 (2023).
- [6] Kishor Bharti, Alba Cervera-Lierta, Thi Ha Kyaw, Tobias Haug, Sumner Alperin-Lea, Abhinav Anand, Matthias Degroote, Hermanni Heimonen, Jakob S. Kottmann, Tim Menke, Wai-Keong Mok, Sukin Sim,

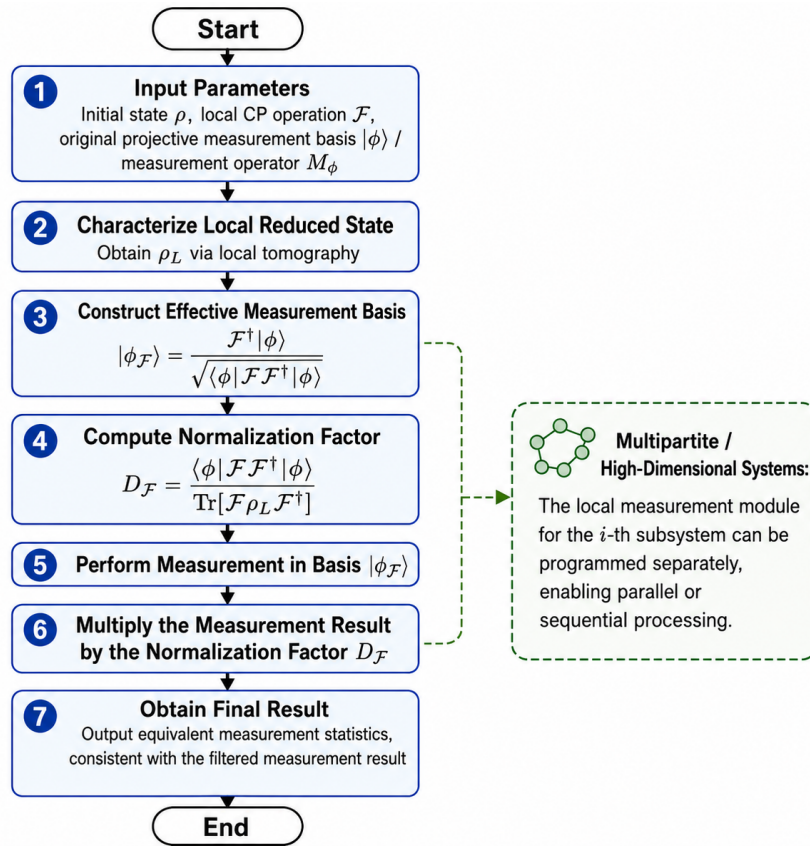


Fig. 5. The process of LMP in a practical experiment.

- Leong-Chuan Kwek, and Alán Aspuru-Guzik, Noisy intermediate-scale quantum algorithms, *Rev. Mod. Phys.* **94**, 015004 (2022).
- [7] Daniel A. Lidar, Review of decoherence-free subspaces, noiseless subsystems, and dynamical decoupling, in *Quantum Information and Computation for Chemistry* (John Wiley, Sons, Ltd, 2014) pp. 295–354.
- [8] Ryszard Horodecki, Paweł Horodecki, Michał Horodecki, and Karol Horodecki, Quantum entanglement, *Rev. Mod. Phys.* **81**, 865 (2009).
- [9] Roope Uola, Ana C. S. Costa, H. Chau Nguyen, and Otfried Gühne, Quantum steering, *Rev. Mod. Phys.* **92**, 015001 (2020).
- [10] Charles H. Bennett, Gilles Brassard, Sandu Popescu, Benjamin Schumacher, John A. Smolin, and William K. Wootters, Purification of noisy entanglement and faithful teleportation via noisy channels, *Phys. Rev. Lett.* **76**, 722–725 (1996).
- [11] David Deutsch, Artur Ekert, Richard Jozsa, Chiara Macchiavello, Sandu Popescu, and Anna Sanpera, Quantum privacy amplification and the security of quantum cryptography over noisy channels, *Phys. Rev. Lett.* **77**, 2818–2821 (1996).
- [12] Daniel Gottesman and Isaac L Chuang, Demonstrating the viability of universal quantum computation using teleportation and single-qubit operations, *Nature* **402**, 390–393 (1999).
- [13] Jian-Wei Pan, Sara Gasparoni, Rupert Ursin, Gregor Weihs, and Anton Zeilinger, Experimental entanglement purification of arbitrary unknown states, *Nature* **423**, 417–422 (2003).
- [14] Yue-Yang Fei, Zhenhuan Liu, Rui Zhang, Zhenyu Cai, Xu-Fei Yin, Yingqiu Mao, Li Li, Nai-Le Liu, Yu-Ao Chen, and Jian-Wei Pan, Experimental quantum channel purification, *Phys. Rev. Lett.* **136**, 110804 (2026).
- [15] Rui Zhang, Yue-Yang Fei, Zhenhuan Liu, Xingjian Zhang, Xu-Fei Yin, Yingqiu Mao, Li Li, Nai-Le Liu, Otfried Gühne, Xiongfeng Ma, et al., Entanglement superactivation in multiphoton distillation networks, arXiv:2510.26290 (2025).
- [16] Jeremy L O’Brien, Akira Furusawa, and Jelena Vučković, Photonic quantum technologies, *Nat. Photonics* **3**, 687–695 (2009).
- [17] Vatsal Srivastav, Natalia Herrera Valencia, Will McCutcheon, Saroch Leedumrongwatthanakun, Sébastien Designolle, Roope Uola, Nicolas Brunner, and Mehul Malik, Quick quantum steering: Overcoming loss and noise with qudits, *Phys. Rev. X* **12**, 041023 (2022).
- [18] G Wendin, Quantum information processing with superconducting circuits: a review, *Rep. Prog. Phys.* **80**, 106001 (2017).
- [19] Nicolas Sangouard, Christoph Simon, Hugues de Riedmatten, and Nicolas Gisin, Quantum repeaters based on atomic ensembles and linear optics, *Rev. Mod. Phys.* **83**, 33–80 (2011).
- [20] Koji Azuma, Kiyoshi Tamaki, and Hoi-Kwong Lo, All-photonic quantum repeaters, *Nat. Commun.* **6**, 6787 (2015).

- [21] Stephanie Wehner, David Elkouss, and Ronald Hanson, Quantum internet: A vision for the road ahead, *Science* **362**, eaam9288 (2018a).
- [22] Dougal Main, Peter Drmota, David P Nadlinger, Ellis M Ainley, Ayush Agrawal, Bethan C Nichol, Raghavendra Srinivas, Gabriel Aranedo, and David M Lucas, Distributed quantum computing across an optical network link, *Nature* **638**, 383–388 (2025).
- [23] Eric Chitambar and Gilad Gour, Quantum resource theories, *Rev. Mod. Phys.* **91**, 025001 (2019).
- [24] Xiao-Min Hu, Cen-Xiao Huang, Yu-Bo Sheng, Lan Zhou, Bi-Heng Liu, Yu Guo, Chao Zhang, Wen-Bo Xing, Yun-Feng Huang, Chuan-Feng Li, and Guang-Can Guo, Long-distance entanglement purification for quantum communication, *Phys. Rev. Lett.* **126**, 010503 (2021).
- [25] Lan Zhou, Cen-Xiao Huang, Yu-Bo Sheng, Yu Guo, Xiao-Min Hu, Yun-Feng Huang, Chuan-Feng Li, Guang-Can Guo, and Bi-Heng Liu, Observation of residual entanglement in entanglement purification, *Phys. Rev. Lett.* **135**, 050801 (2025).
- [26] Yuhang Li, Junjing Xing, Dengke Qu, Huixia Gao, Lei Xiao, Jin-Ming Liu, Yunlong Xiao, and Peng Xue, Temporal asymmetry in entanglement distillation, *Phys. Rev. Lett.* **135**, 170801 (2025).
- [27] Bartosz Regula, Probabilistic transformations of quantum resources, *Phys. Rev. Lett.* **128**, 110505 (2022).
- [28] Nicolas Gisin, Hidden quantum nonlocality revealed by local filters, *Phys. Lett. A* **210**, 151–156 (1996).
- [29] Paul G Kwiat, Salvador Barraza-Lopez, Andre Stefanov, and Nicolas Gisin, Experimental entanglement distillation and hidden non-locality, *Nature* **409**, 1014–1017 (2001).
- [30] Qian-Xi Zhang, Xiao-Xu Fang, and He Lu, Experimental distillation of tripartite quantum steering with an optimal local filtering operation, *Photon. Res.* **12**, 552–562 (2024a).
- [31] Xiao-Xu Fang, Gelo Noel M. Tabia, Kai-Siang Chen, Yeong-Cherng Liang, and He Lu, Experimental single-copy distillation of quantumness from higher-dimensional entanglement, *Phys. Rev. Lett.* **134**, 150201 (2025).
- [32] Tanumoy Pramanik, Young-Wook Cho, Sang-Wook Han, Sang-Yun Lee, Yong-Su Kim, and Sung Moon, Revealing hidden quantum steerability using local filtering operations, *Phys. Rev. A* **99**, 030101 (2019).
- [33] Jason M. Dominy, Alireza Shabani, and Daniel A. Lidar, A general framework for complete positivity, *Quantum Inf. Process.* **15**, 465–494 (2016).
- [34] R. V. Nery, M. M. Taddei, P. Sahium, S. P. Walborn, L. Aolita, and G. H. Aguilar, Distillation of quantum steering, *Phys. Rev. Lett.* **124**, 120402 (2020).
- [35] Huan-Yu Ku, Chung-Yun Hsieh, Shin-Liang Chen, Yueh-Nan Chen, and Costantino Budroni, Complete classification of steerability under local filters and its relation with measurement incompatibility, *Nat. Commun.* **13**, 4973 (2022).
- [36] Yang Liu, Kaimin Zheng, Haijun Kang, Dongmei Han, Meihong Wang, Lijian Zhang, Xiaolong Su, and Kunchi Peng, Distillation of gaussian einstein-podolsky-rosen steering with noiseless linear amplification, *npj Quantum Inf.* **8**, 38 (2022).
- [37] Ze-Yan Hao, Yan Wang, Jia-Kun Li, Yu Xiang, Qiong-Yi He, Zheng-Hao Liu, Mu Yang, Kai Sun, Jin-Shi Xu, Chuan-Feng Li, and Guang-Can Guo, Filtering one-way einstein-podolsky-rosen steering, *Phys. Rev. A* **109**, 022411 (2024).
- [38] Ryuji Takagi, Xiao Yuan, Bartosz Regula, and Mile Gu, Virtual quantum resource distillation: General framework and applications, *Phys. Rev. A* **109**, 022403 (2024).
- [39] Xiao Yuan, Bartosz Regula, Ryuji Takagi, and Mile Gu, Virtual quantum resource distillation, *Phys. Rev. Lett.* **132**, 050203 (2024).
- [40] Ting Zhang, Yukun Zhang, Lu Liu, Xiao-Xu Fang, Qian-Xi Zhang, Xiao Yuan, and He Lu, Experimental virtual distillation of entanglement and coherence, *Phys. Rev. Lett.* **132**, 180201 (2024b).
- [41] Neil Dowling, Pavel Kos, and Xhek Turkeshi, Magic resources of the heisenberg picture, *Phys. Rev. Lett.* **135**, 050401 (2025).
- [42] See Supplemental Material for details of local program operation, experimental setup, criteria of quantum entanglement and steering in bipartite and tripartite systems.
- [43] Alessandro Fedrizzi, Thomas Herbst, Andreas Poppe, Thomas Jennewein, and Anton Zeilinger, A wavelength-tunable fiber-coupled source of narrowband entangled photons, *Opt. Express* **15**, 15377–15386 (2007).
- [44] Ya Xiao, Xiang-Jun Ye, Kai Sun, Jin-Shi Xu, Chuan-Feng Li, and Guang-Can Guo, Demonstration of multi-setting one-way einstein-podolsky-rosen steering in two-qubit systems, *Phys. Rev. Lett.* **118**, 140404 (2017).
- [45] Daniel Cavalcanti, Paul Skrzypczyk, GH Aguilar, Ranieri V Nery, PH Souto Ribeiro, and SP Walborn, Detection of entanglement in asymmetric quantum networks and multipartite quantum steering, *Nat. Commun.* **6**, 7941 (2015).
- [46] Daniel F. V. James, Paul G. Kwiat, William J. Munro, and Andrew G. White, Measurement of qubits, *Phys. Rev. A* **64**, 052312 (2001).
- [47] William K. Wootters, Entanglement of formation of an arbitrary state of two qubits, *Phys. Rev. Lett.* **80**, 2245–2248 (1998).
- [48] Yi-Zheng Zhen, Yu-Lin Zheng, Wen-Fei Cao, Li Li, Zeng-Bing Chen, Nai-Le Liu, and Kai Chen, Certifying einstein-podolsky-rosen steering via the local uncertainty principle, *Phys. Rev. A* **93**, 012108 (2016).
- [49] A. Acín, D. Bruß, M. Lewenstein, and A. Sanpera, Classification of mixed three-qubit states, *Phys. Rev. Lett.* **87**, 040401 (2001).
- [50] J. I. Cirac, P. Zoller, H. J. Kimble, and H. Mabuchi, Quantum state transfer and entanglement distribution among distant nodes in a quantum network, *Phys. Rev. Lett.* **78**, 3221–3224 (1997).
- [51] L-M Duan, Mikhail D Lukin, J Ignacio Cirac, and Peter Zoller, Long-distance quantum communication with atomic ensembles and linear optics, *Nature* **414**, 413–418 (2001).
- [52] Stephanie Wehner, David Elkouss, and Ronald Hanson, Quantum internet: A vision for the road ahead, *Science* **362**, eaam9288 (2018b).
- [53] Filippo Caruso, Vittorio Giovannetti, Cosmo Lupo, and Stefano Mancini, Quantum channels and memory effects, *Rev. Mod. Phys.* **86**, 1203–1259 (2014).
- [54] Fernando E. Becerra, Jian Fan, and Alan Migdall, Implementation of generalized quantum measurements for unambiguous discrimination of multiple non-orthogonal coherent states, *Nat. Commun.* **4**, 2028 (2013).
- [55] Reinhold A. Bertlmann and Nicolai Friis, Quantum channels and quantum operations, in *Modern Quantum The-*

- ory: From Quantum Mechanics to Entanglement and Quantum Information (Oxford University Press, Oxford, UK, 2023).
- [56] Valerio Scarani, Helle Bechmann-Pasquinucci, Nicolas J. Cerf, Miloslav Dušek, Norbert Lütkenhaus, and Momtchil Peev, The security of practical quantum key distribution, *Rev. Mod. Phys.* **81**, 1301–1350 (2009).
- [57] Neng-Chun Chiu, Elias C Trapp, Jinen Guo, Mohamed H Abobeih, Luke M Stewart, Simon Hollerith, Pavel L Stroganov, Marcin Kalinowski, Alexandra A Geim, Simon J Evered, et al., Continuous operation of a coherent 3,000-qubit system, *Nature* **646**, 1075–1080 (2025).
- [58] Kai Sun, Ze-Yan Hao, Yan Wang, Jia-Kun Li, Xiao-Ye Xu, Jin-Shi Xu, Yong-Jian Han, Chuan-Feng Li, and Guang-Can Guo, Optical demonstration of quantum fault-tolerant threshold, *Light Sci. Appl.* **11**, 203 (2022).